Med Chem Res (2014) 23:2080–2092
DOI 10.1007/s00044-013-0786-y

MEDICINAL CHEMISTRY RESEARCH

ORIGINAL RESEARCH

Synthesis, biological evaluation, and molecular modeling of (*E*)-2-aryl-5-styryl-1,3,4-oxadiazole derivatives as acetylcholine esterase inhibitors

Ahmed Kamal · Anver Basha Shaik · G. Narender Reddy · C. Ganesh Kumar · Joveeta Joseph · G. Bharath Kumar · Uppula Purushotham · G. Narahari Sastry

Received: 21 February 2013 / Accepted: 10 September 2013 / Published online: 6 October 2013

Abstract A library of 2,5-disubstituted 1,3,4-oxadiazole derivatives of (*E*)-2-aryl-5-(3,4,5-trimethoxystyryl)-1,3,4-oxadiazoles **4**(**a**–**o**) and (*E*)-2-aryl-5-(2-benzo[d][1,3]dioxol-5-yl)vinyl)-1,3,4-oxadiazoles **5**(**a**–**q**) were synthesized and evaluated for their in vitro acetylcholinesterase (AChE) inhibitory activity. All the synthesized compounds exhibited moderate to good inhibitory activity toward the AChE enzyme. Among the oxadiazole derivatives examined, compounds **4a**, **4g**, **5c**, and **5m** (IC_{50} values of 24.89, 13.72, 37.65, and 19.63 μM, respectively) were found to be promising inhibitors of AChE. Molecular protein–ligand docking studies were examined for these compounds using GOLD docking software and their binding conformations were determined and the simultaneous interactions mode was also established for the potent derivatives.

Keywords 2-Aryl-5-styryl-1,3,4-oxadiazoles · Derivatives · Acetylcholine esterase inhibitors · Molecular modeling

Introduction

Alzheimer's disease (AD), the most common neurodegenerative disorder associated with aging, is accompanied by severe deficiency in choline acetyltransferase (ChAT) activity in the hippocampus and cerebral cortex. A significant correlation has been found between a decrease in cortical cholinergic activity and the deterioration of mental test scores in patients suffering from AD. Therefore, potentiation of central cholinergic activity has been proposed as a possible therapeutic approach to improve cognitive function in AD patients (Bartus *et al*., 1982). Among the most promising strategies is the elevation of the brain concentration of neurotransmitter acetylcholine (ACh) by centrally acting acetylcholinesterase (AChE, EC 3.1.1.7) inhibitors. During the past decade, several cholinergic drugs have been launched in the market, including the synthetic compounds, Tacrine (Davis and Powchik, 1995), Galanthamine (Rainer, 1997), Donepezil (Kawakami *et al*., 1996), and Rivastigmine (Prous *et al*., 1996). It has been reported that use of these drugs produced significant cognitive improvement (Wagstaff and McTavish, 1994; Bartus *et al*., 1982; Johansson *et al*., 1996). However, a major drawback on their widespread use as a general therapy exhibited undesirable side effects such as hepatotoxicity which impose severe dose limits.

The comprehensive study of the AChE inhibitor complexes by X-ray crystallography indicated that AChE possessed a narrow gorge with two separate ligand binding sites, an acylation site (active site) and a peripheral site which is also called peripheral anionic site. Simultaneous binding to the catalytic anionic subsite and the peripheral anionic site is responsible for the enhanced binding of gorge-spanning ligands, such as galanthamine (Fig. 1a) and donepezil (Fig. 1b). Recent biochemical studies have shown that the peripheral anionic site is also implicated in promoting aggregation of the beta-amyloid (Aβ) peptide responsible for the neurodegenerative process in AD (Alvarez *et al*., 1997, 1998; De Ferrari *et al*., 2001). Thus, the design of inhibitors interacting with the peripheral anionic site is of potential interest for the treatment of AD (Andreani *et al*., 2001).

A. Kamal (✉) · A. B. Shaik · G. N. Reddy · C. G. Kumar · J. Joseph · G. B. Kumar
Chemical Biology Laboratory, Medicinal Chemistry and Pharmacology Division, CSIR-Indian Institute of Chemical Technology, Hyderabad 500007, India
e-mail: ahmedkamal@iict.res.in

U. Purushotham · G. N. Sastry
Molecular Modeling Group, CSIR-Indian Institute of Chemical Technology, Hyderabad 500007, India

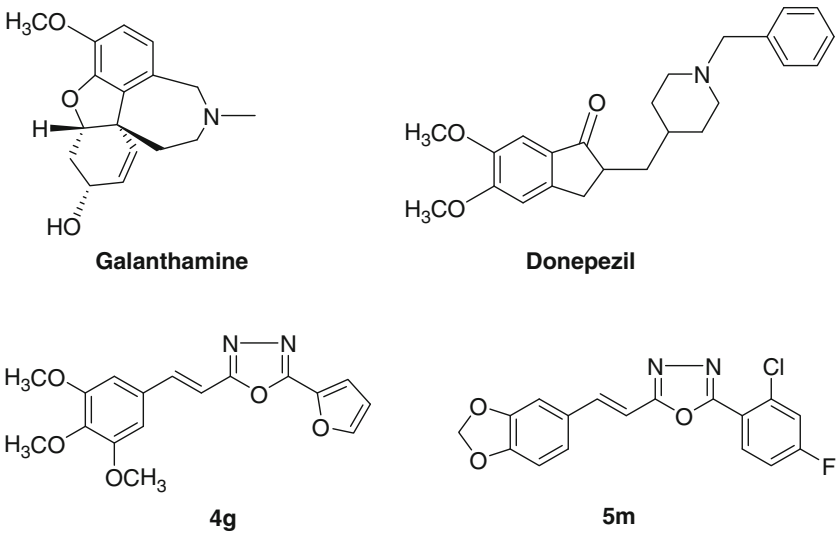

Fig. 1 Chemical structures of galanthamine, donepezil, (*E*)-2-(2-furan-2-yl)-5-(3,4,5-trimethoxystyryl)-1,3,4-oxadiazole (**4g**), and (*E*)-2-(2-benzo[d][1,3]dioxol-5-yl)vinyl)-5-(2-chloro-4-fluorophenyl)-1,3,4-oxadiazole (**5m**)

Heterocyclic compounds containing the five-membered oxadiazole nucleus possess a diversity of useful biological effects. Differently 2,5-disubstituted oxadiazole moieties have also been reported to have other interesting activities such as analgesic (Narayana *et al*., 2005; Alam *et al*., 2011), antimicrobial (Gaonkar *et al*., 2006), anticonvulsant (Zarghi *et al*., 2005), and anti-hepatitis B viral activities (Tan *et al*., 2006). In particular, oxadiazole derivatives bearing the 1,3,4-oxadiazole nucleus are known to have unique anti-edema and anti-inflammatory activities (Narayana *et al*., 2005; Alam *et al*., 2011) and also exhibit AChE inhibitory activity (Al-Kazzaz *et al*., 2011) and central nervous system depressant activity (Singh *et al*., 2012). However, docking studies have not been reported for these aforementioned derivatives. Considering these facts, we have synthesized (*E*)-2-aryl-5-styryl-1,3,4-oxadiazole derivatives **4**(**a**–**o**) and **5**(**a**–**q**), which are hybrids containing both the styryl and oxadiazole moieties, that contain trimethoxy phenyl and 3,4-(methylenedioxy) phenyl groups (Fig. 1—4g, 5m) by facile procedures described previously (Shi *et al*., 2001; Lee *et al*., 2010; Bhattacharya *et al*., 2010; Jha *et al*., 2010). Additionally, their effect on AChE inhibition was investigated and docking simulations were also carried out on the three-dimensional structures of AChE, to understand the structural requirements for the recognition between the AChE and the ligands.

Materials and methods

Synthesis and structural characterization

All chemicals were purchased from different companies like Sigma-Aldrich, St. Louis, MO, USA, Alfa Aesar, Johnson Matthey Company, Ward Hill, MA, USA, and Spectrochem Pvt. Ltd, Mumbai, India and were used without further purification. Reactions were monitored by TLC, performed on silica gel glass plates containing 60 GF-254, and visualization on TLC was achieved by UV light or iodine indicator. Column chromatography was performed with Merck 60–120 mesh silica gel. The NMR spectra were recorded on Gemini Varian-VXR-Unity (200 MHz) or Bruker UXNMR/XWIN-NMR (300 MHz) instruments. Chemical shifts (δ) are reported in ppm relative to the peak for tetramethylsilane (TMS) as an internal standard, and coupling constants are reported in Hertz (Hz). IR spectra are recorded on Perkin-Elmer model 683 or 1310 spectrometer with sodium chloride optics. ESI spectra were recorded on Micro mass, Quattro LC using ESI^+ software with capillary voltage of 3.98 kV and ESI mode positive ion trap detector. Melting points were determined with an Electro thermal melting point apparatus and are uncorrected.

General procedure for the synthesis of carboxylic acid ester **7**(**a**–**q**)

To 10 ml of ethanol, (1.0 mol) of carboxylic acid **6**(**a**–**q**) was added in a 100-ml round-bottomed flask. To this, catalytic amount of concentrated H_2SO_4 was added at room temperature and was heated under reflux with continuous stirring for 3–4 h at 85 °C. After 3 h, the reaction was monitored by TLC using ethyl acetate and hexane (3:7) system. Stirring was continued until TLC indicated the completion of reaction. Then the reaction mixture was allowed to reach the room temperature. Ethanol was distilled off under reduced pressure and the residue was dissolved in water and then extracted twice with ethyl acetate. The combined organic solutions were washed with saturated $NaHCO_3$ solution, finally washed with water and

dried over anhydrous Na_2SO_4. The solvent was removed under vacuum to get carboxylic acid ester, which is an oily liquid. The ester obtained was taken as such in the next step of synthesis.

General procedure for the synthesis of acid hydrazides **8**(**a**–**q**)

To the carboxylic acid ester (1.0 mol) obtained in step I, 10 ml of ethanol was added in a 100-ml round-bottomed flask. To this, hydrazine hydrate (4.0 mol) was added at room temperature and then heated under reflux conditions with continuous stirring for 3–4 h at 85 °C. After 3 h, the reaction was monitored by TLC using ethyl acetate and hexane (1:1) system. Stirring was continued until TLC indicated the completion of reaction. The reaction was allowed to reach the room temperature. Ethanol was distilled off under reduced pressure. The residue was dissolved in water and extracted twice with ethyl acetate, dried over anhydrous Na_2SO_4 and the solvent was removed under reduced pressure to afford the compound **8**(**a**–**q**) as crystalline solid. The hydrazide obtained was taken as such in the next step of synthesis.

General procedure for the synthesis of (*E*)-2-aryl-5-styryl-1,3,4-oxadiazoles **4**(**a**–**o**) and **5**(**a**–**q**)

To an equimolar mixture, (0.002 mol) of 3,4,5-trimethoxycinnamic acid or 3,4-(methyledioxy)cinnamic acid, an appropriate acid hydrazide in 7–8 ml of phosphorus oxychloride was added and the reaction mixture was refluxed at 110 °C for 5–6 h. After completion of reaction, the mixture was poured onto crushed ice (40 g) and neutralized with saturated $NaHCO_3$ solution. The product so obtained was extracted twice with ethyl acetate and dried on anhydrous Na_2SO_4. The solvent was removed under reduced pressure to get the crude product. This residue was further purified by column chromatography by using ethyl acetate and hexane to yield pure solid (*E*)-2-aryl-5-styryl-1,3,4-oxadiazoles **4**(**a**–**o**) and **5**(**a**–**q**).

*(E)-2-phenyl-5-(3,4,5-trimethoxystyryl)-1,3,4-oxadiazole (**4a**)*

Pale yellow solid; (yield 620 mg, 87.3 %): $R_f = 0.6$ (50 % ethyl acetate/hexane); mp: 150–153 °C; ^{1}H NMR (300 MHz, $CDCl_3$); δ 3.89 (s, 3H, –OCH_3), 3.92 (s, 6H, –OCH_3), 6.79 (s, 2H, Ar*H*), 7.00 (d, 1H, $J = 15.8$ Hz, *trans*-C*H*=C*H*), 7.48–7.56 (m, 4H, Hz, Ar*H*, $J = 15.8$ Hz, *trans*-C*H*=C*H*), 8.09–8.15 (m, 2H, Ar*H*); ^{13}C NMR (75 MHz, $CDCl_3$): δ 56.0 (O*C*H$_3$), 60.9 (O*C*H$_3$), 104.6 (Ar–*C*), 109.2 (Ar–*C*), 123.7 (H*C*=CH), 126.8, 128.9, 130.2(Ar–*C*), 131.6 (H*C*=CH), 138.7 (*C*–OCH$_3$), 153.4 (*C*–OCH$_3$), 164.1(*C*=N), ppm; IR (KBr) (ν_{max}/cm^{-1}): $\nu = 3449$, 2925, 2833, 1641, 1583, 1526, 1502, 1452, 1418, 1331, 1245, 1128 cm^{-1}; MS (ESI): *m/z* 339[M+1]; HR-MS (ESI) for $C_{19}H_{19}N_2O_4$ calculated *m/z*: 339.1344, found *m/z*: 339.1332.

*(E)-2-p-tolyl-5-(3,4,5-trimethoxystyryl)-1,3,4-oxadiazole (**4b**)*

Pale yellow-colored solid; (yield 550 mg, 79.8 %): $R_f = 0.4$ (50 % ethyl acetate/hexane); mp: 134–136 °C; ^{1}H NMR (400 MHz, $CDCl_3$); δ 2.45 (s, 3H, –CH_3), 3.86 (s, 3H, –OCH_3), 3.91 (s, 6H, –OCH_3), 6.76 (s, 2H, Ar*H*), 6.98 (d, 1H, $J = 16.4$ Hz, *trans*-C*H*=C*H*), 7.29 (d, 2H, $J = 8.1$ Hz, Ar*H*), 7.48 (d, 1H, $J = 16.4$ Hz, *trans*-C*H*=C*H*), 7.98 (d, 2H, $J = 8.1$ Hz, Ar*H*); ^{13}C NMR (75 MHz, $CDCl_3$): δ 21.6(*C*H$_3$), 56.1(O*C*H$_3$), 61.0 (O*C*H$_3$), 104.5, 109.4 (Ar–*C*), 121.0, 126.8 (Ar–*C*), 129.7 (H*C*=CH), 138.5 (H*C*=CH), 142.3(*C*–OCH$_3$), 153.5(*C*–OCH$_3$), 164.0 (*C*=N) ppm; IR (KBr) (ν_{max}/cm^{-1}): $\nu = 3423$, 3046, 2936, 1633, 1579, 1498, 1331, 1243, 1126 cm^{-1}; MS (ESI): *m/z* 353 [M+1]; HR-MS (ESI) *m/z* for $C_{20}H_{18}N_2O_4$ calculated *m/z*: 353.1518, found *m/z*: 353.1512.

*(E)-2-(2,4-dichlorophenyl)l-5-(3,4,5-trimethoxystyryl)-1,3,4-oxadiazole (**4c**)*

Yellow-colored solid; (yield 690 mg, 80.7 %): $R_f = 0.5$ (50 % ethyl acetate/hexane); mp: 154–156 °C; ^{1}H NMR (300 MHz, $CDCl_3$); δ 3.86 (s, 3H, –OCH_3), 3.91 (s, 6H, –OCH_3), 6.76 (s, 2H, Ar*H*), 6.98 (d, 1H, $J = 16.4$ Hz, *trans*-C*H*=C*H*), 7.39–7.42 (m, 1H, Ar*H*), 7.49 (d, 1H, $J = 16.4$ Hz, *trans*-C*H*=C*H*), 7.99 (d, 1H, $J = 1.8$ Hz, Ar*H*), 8.07 (d, 1H, $J = 8.4$ Hz, Ar*H*); ^{13}C NMR (75 MHz, $CDCl_3$): δ 56.1 (O*C*H$_3$), 60.9 (O*C*H$_3$), 104.6(Ar–*C*), 108.8(Ar–*C*), 121.5(Ar–*C*), 127.5(H*C*=CH), 130.0, 131.1, 131.7(Ar–*C*), 133.6 (H*C*=CH), 138.0(Ar–*C*), 139.5(*C*–OCH$_3$), 153.4(*C*–OCH$_3$), 161.6(*C*=N), 164.1(*C*=N) ppm; IR (KBr) (ν_{max}/cm^{-1}): $\nu = 3385$, 2925, 1635, 1584, 1507, 1454, 1413, 1334, 1241 cm^{-1}; MS (ESI): *m/z* 407 [M+1]; HR-MS (ESI) *m/z* for $C_{19}H_{17}N_2O_4Cl_2$ calculated *m/z*: 407.0565, found *m/z*: 407.0556.

*(E)-2-(2-chloropyridin-3-yl)-5-(3,4,5-trimethoxystyryl)-1,3,4-oxadiazole (**4d**)*

Yellow-colored solid; (yield 410 mg, 52.2 %): $R_f = 0.4$ (50 % ethyl acetate/hexane); mp: 141–143 °C; ^{1}H NMR (200 MHz, $CDCl_3$); δ 3.87 (s, 3H, –OCH_3), 3.92 (s, 6H, –OCH_3), 6.76 (d, 2H, $J = 7.5$ Hz, Ar*H*), 6.98 (d, 1H, $J = 15.8$ Hz, *trans*-C*H*=C*H*), 7.40–7.45 (m, 1H, Ar*H*), 7.55 (d, 1H, $J = 15.8$ Hz, *trans*-C*H*=C*H*), 8.46–8.57 (m, 2H, Ar*H*); ^{13}C NMR (75 MHz, $CDCl_3$): δ 56.1 (O*C*H$_3$), 60.9 (O*C*H$_3$), 104.8, 105.4, 108.6, 120.3 (Ar–*C*), 122.4 (H*C*=CH), 130.3 (H*C*=CH), 139.7(*C*–OCH$_3$), 139.9, 140.1,

148.9 (Ar–*C*), 151.7 (Ar–*C*–Cl), 153.4 (Ar–*C*), 153.5 (*C*–OCH_3), 160.8 (*C*=N), 165.2 (*C*=N) ppm; IR (KBr) (ν_{max}/cm^{-1}): ν = 3424, 3060, 2930, 1740, 1642, 1583, 1462, 1239, 1134, 962 cm^{-1}; MS (ESI) *m/z* 374; HR-MS (ESI) *m/z* for $C_{18}H_{17}N_3O_4Cl$ calculated *m/z*: 374.0907, found *m/z*: 374.0908.

*(E)-2-(2-bromophenyl)-5-(3,4,5-trimethoxystyryl)-1,3,4-oxadiazole (**4e**)*

Yellow-colored solid; (yield 535 mg, 161.1 %): R_f = 0.5 (50 % ethyl acetate/hexane); mp: 122–125 °C; ^{1}H NMR (300 MHz, $CDCl_3$); δ 3.86 (s, 3H, –O*C*H_3), 3.91 (s, 6H, –O*C*H_3), 6.89 (d, 1H, J = 8.3 Hz, Ar*H*), 6.93 (s, 1H, Ar*H*), 7.41–7.55 (m, 4H, J = 7.0 Hz, Ar*H*, J = 15.8 Hz, *trans*-C*H*=C*H*), 8.01–8.12 (m, 2H, Ar*H*); ^{13}C NMR (75 MHz, $CDCl_3$): δ 56.0 (O*C*H_3), 60.8 (O*C*H_3), 104.5, 109.0, 109.1, 121.3(Ar–*C*), 125.0 (H*C*=CH), 126.8, 127.5, 128.9, 130.1, 131.4, 131.6, 132.3(Ar–*C*), 134.5(H*C*=CH), 138.7(*C*–OCH_3), 139.2(Ar–*C*–Br), 153.4(*C*–OCH_3), 161.8(*C*=N), 164.3(*C*=N) ppm; IR (KBr) (ν_{max}/cm^{-1}): ν = 3455, 3051, 2989, 2832, 1973, 1740, 1704, 1636, 1584, 1524, 1460, 1417, 1329, 1244, 1181, 1131 cm^{-1}; MS (ESI) *m/z* 417; HR-MS (ESI) *m/z* for $C_{19}H_{18}N_2O_4Br$ calculated *m/z*: 417.0449, found *m/z*: 417.0452.

*(E)-2-(2-benzofuran-2-yl)-5-(3,4,5-trimethoxystyryl)-1,3,4-oxadiazole (**4f**)*

Yellow-colored solid; (yield 715 mg, 90.05 %): R_f = 0.4 (50 % ethyl acetate/hexane); mp: 189–190 °C; ^{1}H NMR (200 MHz, $CDCl_3$); δ 3.87 (s, 3H, –O*C*H_3), 3.92 (s, 6H, –O*C*H_3), 6.79 (s, 1H, Ar*H*), 6.98 (d, 1H, J = 16.0 Hz, *trans*-C*H*=C*H*), 7.28–7.36 (m, 2H, J = 8.8 Hz, Ar*H*), 7.40–7.46 (m, 1H, J = 7.7 Hz, Ar*H*), 7.56–7.65 (m, 3H, J = 7.7 Hz Ar*H*, J = 16.0 Hz *trans*-C*H*=C*H*), 7.69 (d, 1H, J = 7.5 Hz, Ar*H*); ^{13}C NMR (75 MHz, $CDCl_3$): δ 56.1 (O*C*H_3), 60.9 (O*C*H_3), 104.7 (Ar–*C*),108.5 (Ar–*C*), 110.1, 111.9, 122.2 (Ar–*C*), 124.0 (H*C*=CH), 127.2(Ar–*C*), 130.0 (H*C*=CH), 140.5 (*C*–*O*), 139.6 (*C*–OCH_3), 153.5 (*C*–OCH_3), 155.6 (*C*–*O*), 157.1(*C*=N), 164.1(*C*=N) ppm; IR (KBr) (ν_{max}/cm^{-1}): ν = 3423, 3050, 2928, 2834, 1638, 1583, 1453, 1420, 1247, 1132, 972 cm^{-1}; MS (ESI) *m/z*: 379; HR-MS (ESI) *m/z* for $C_{21}H_{19}N_2O_5$ calculated *m/z*: 379.1293, found *m/z*: 379.1281.

*(E)-2-(2-furan-2-yl)-5-(3,4,5-trimethoxystyryl)-1,3,4-oxadiazole (**4g**)*

Light yellow-colored solid; (yield 410 mg, 87.1 %): R_f = 0.5 (50 % ethyl acetate/hexane); mp: 154–157 °C; ^{1}H NMR (300 MHz, $CDCl_3$ + DMSO-d_6); δ 3.86 (s, 3H, –O*C*H_3), 3.91 (s, 6H, –O*C*H_3), 6.75 (s, 2H, Ar*H*), 6.93 (d, 1H, J = 16.0 Hz, *trans*-C*H*=C*H*), 6.96–7.00 (s, 1H, Ar*H*), 7.46 (d, 1H, J = 16.4 Hz, *trans*-C*H*=C*H*), 7.55 (s, 1H, Ar*H*), 8.12 (s, 1H, Ar*H*); ^{13}C NMR (75 MHz, $CDCl_3$ + DMSO-d_6): δ 56.0 (O*C*H_3), 60.9 (O*C*H_3), 104.5 (Ar–*C*), 108.4, 109.0, 111.6 (Ar–*C*), 130.2 (H*C*=CH), 139.7 (*C*–*O*), 138.6 (*C*–OCH_3), 143.4 (Ar–*C*), 144.4 (*C*–*O*), 153.4 (*C*–OCH_3), 159.0 (*C*=N), 163.5 (*C*=N) ppm; IR (KBr) (ν_{max}/cm^{-1}): ν = 3442, 3033, 2945, 2834, 1653, 1582, 1419, 1240, 1162, 1126, 975 cm^{-1}; MS (ESI) *m/z* 329; HR-MS (ESI) *m/z* for $C_{17}H_{17}N_2O_5$ calculated *m/z*: 329.1137, found *m/z*: 329.1127.

*(E)-2-(4-nitrophenyl)-5-(3,4,5-trimethoxystyryl)-1,3,4-oxadiazole (**4h**)*

Yellow-colored solid; (yield 425 mg, 52.84 %): R_f = 0.4 (50 % ethyl acetate/hexane); mp: 183–185 °C; ^{1}H NMR (400 MHz, $CDCl_3$); δ 3.87 (s, 3H, –O*C*H_3), 3.92 (s, 6H, –O*C*H_3), 6.78 (s, 2H, Ar*H*), 6.97 (d, 1H, J = 16.4 Hz, *trans*-C*H*=C*H*–), 7.56 (d, 1H, J = 16.4 Hz, *trans*-C*H*=C*H*), 8.29 (d, 2H, J = 8.6 Hz, Ar*H*), 8.38 (d, 2H, J = 7.5 Hz, Ar*H*); ^{13}C NMR (75 MHz, $CDCl_3$ + DMSO-d6): δ 56.1 (O*C*H_3), 60.9 (O*C*H_3), 104.7, 108.4, 121.5(Ar–*C*), 125.4 (H*C*=CH), 126.0, 129.9, 130.3 (Ar–*C*), 132.4 (H*C*=CH), 139.9 (*C*–OCH_3), 148.5 (*C*–NO_2), 153.5 (*C*–OCH_3), 161.9 (*C*=N), 164.8 (*C*=N) ppm; IR (KBr) (ν_{max}/cm^{-1}): ν = 3426, 2926, 1633, 1584, 1555, 1529, 1456, 1413, 1332, 1243, 1156, 1123 cm^{-1}; MS (ESI) *m/z*: 384; HR-MS (ESI) *m/z* for $C_{19}H_{18}N_3O_6$ calculated *m/z*: 384.1195, found *m/z*: 384.1185.

*(E)-2-(3,4,5-trimethoxyphenyl)-5-(3,4,5-trimethoxystyryl)-1,3,4-oxadiazole (**4i**)*

Light yellow-colored solid; (yield 310 mg, 61.19 %): R_f = 0.4 (50 % ethyl acetate/hexane); mp: 153–155 °C; ^{1}H NMR (300 MHz, $CDCl_3$ + DMSO-d_6); δ 3.86 (s, 3H, –O*C*H_3), 3.90 (s, 3H, –O*C*H_3), 3.91 (s, 6H, –O*C*H_3), 3.97 (s, 6H, –O*C*H_3), 6.77 (s, 2H, Ar*H*), 6.95 (d, 1H, J = 16.6 Hz, *trans*-C*H*=C*H*–), 7.29 (d, 2H, J = 3.7 Hz, Ar*H*), 7.49 (d, 1H, J = 16.6 Hz, *trans*-C*H*=C*H*–); ^{13}C NMR (75 MHz; $CDCl_3$ + DMSO-d_6): δ 56.1 (O*C*H_3), 60.9 (O*C*H_3), 104.2, 104.6, 109.1 (Ar–*C*), 118.8 (H*C*=CH), 130.2 (H*C*=CH), 138.6, 138.7(*C*–OCH_3), 139.8, 141.2 (Ar–*C*), 153.4, 153.6 (*C*–OCH_3), 163.6 (*C*=N), 163.8 (*C*=N) ppm; IR (KBr) (ν_{max}/cm^{-1}): ν = 3419, 2928, 2835, 1641, 1584, 1497, 1458, 1417, 1328, 1238, 1180, 1124 cm^{-1}; MS (ESI) *m/z*: 428; HR-MS (ESI) *m/z* for $C_{22}H_{24}N_2O_7Na$ calculated *m/z*:451.1481, found *m/z*: 451.1494.

*(E)-2-(3-nitrophenyl)-5-(3,4,5-trimethoxystyryl)-1,3,4-oxadiazole (**4j**)*

Yellow-colored solid; (yield 410 mg, 50.97 %): R_f = 0.4 (50 % ethyl acetate/hexane); mp: 156–158 °C; ^{1}H NMR

(300 MHz, $CDCl_3$); δ 3.89 (s, 3H, –OCH_3), 3.92 (s, 6H, –OCH_3), 6.82 (s, 2H, Ar*H*), 6.99 (d, 1H, $J = 16.4$ Hz, *trans*-C*H*=C*H*), 7.61 (d, 1H, $J = 16.4$ Hz, *trans*-C*H*=C*H*), 7.74 (t, 1H, $J = 7.9$ Hz, Ar*H*), 8.39–8.43 (m, 1H, Ar*H*), 8.51 (d, 1H, $J = 7.7$ Hz, Ar*H*), 8.89 (s, 1H, Ar*H*); ^{13}C NMR (75 MHz, $CDCl_3$): δ 56.1 (O*C*H_3), 60.9 (O*C*H_3), 104.7, 108.4, 121.5 (Ar–*C*), 125.4 (H*C*=CH), 126.0, 129.9, 130.3(Ar–*C*), 132.4 (H*C*=CH), 139.9 (*C*–OCH_3), 148.5 (*C*–NO_2), 153.5 (*C*–OCH_3), 161.9 (*C*=N), 164.8 (*C*=N) ppm; IR (KBr) (ν_{max}/cm^{-1}): $\nu = 3423$, 2925, 1733, 1638, 1584, 1523, 1461, 1419, 1339, 1244, 1127 cm^{-1}; MS (ESI) *m/z*: 384; HR-MS (ESI) *m/z* for $C_{19}H_{18}N_3O_6$ calculated *m/z*: 384.1195, found *m/z*: 384.1185.

*(E)-2-(2-chlorophenyl)-5-(3,4,5-trimethoxystyryl)-1,3,4-oxadiazole (**4k**)*

Yellow-colored solid; (yield 516 mg, 52.0 %): $R_f = 0.5$ (50 % ethyl acetate/hexane); mp: 144–146 °C; ^{1}H NMR (200 MHz, $CDCl_3$); δ 3.89 (s, 3H, –OCH_3), 3.93 (s, 6H, –OCH_3), 6.79 (s, 2H, Ar*H*), 6.98 (d, 1H, $J = 16.8$ Hz, *trans*-C*H*=C*H*–), 7.41–7.58 (m, 4H, ArH, $J = 16.8$ Hz, *trans*-C*H*=C*H*–), 8.09 (d, 1H, $J = 7.9$ Hz, Ar*H*) ^{13}C NMR (75 MHz, $CDCl_3$ + DMSO-d_6): δ 56.1 (O*C*H_3), 60.9 (O*C*H_3), 104.6, 109.0 (Ar–*C*), 127.0 (H*C*=CH), 130.1, 131.0, 131.2 (Ar–*C*), 132.3 (H*C*=CH), 132.9 (Ar*C*–Cl), 139.2 (Ar–*C*), 139.8 (*C*–OCH_3), 153.4 (*C*–OCH_3), 162.2 (*C*=N), 164.5 (*C*=N) ppm; IR (KBr) (ν_{max}/cm^{-1}): $\nu = 3429$, 2689, 2927, 2834, 2365, 1741, 1636, 1585, 1525, 1447, 1416, 1330, 1244, 1132 cm^{-1}; MS (ESI) *m/z* 472; HR-MS (ESI) *m/z* for $C_{19}H_{18}N_2O_4Cl$ calculated *m/z*: 373.0955, found *m/z*: 373.0946.

*(E)-2-(2-chloro-4-fluorophenyl)-5-(3,4,5-trimethoxystyryl)-1,3,4-oxadiazole (**4l**)*

Light yellow-colored solid; (yield 328 mg, 50.0 %): $R_f = 0.5$ (50 % ethyl acetate/hexane); mp: 160–162 °C; ^{1}H NMR (300 MHz, $CDCl_3$ + DMSO-d_6); δ 3.86 (s, 3H, –OCH_3), 3.92 (s, 6H, –OCH_3), 6.76 (s, 2H, Ar*H*), 6.98 (d, 1H, $J = 16.4$ Hz, *trans*-C*H*=C*H*–), 7.12–7.19 (m, 1H, Ar*H*), 7.30–7.34 (m, 1H, Ar*H*), 7.48 (d, 1H, $J = 16.4$ Hz *trans*-C*H*=C*H*), 8.11–8.17 (m, 1H, Ar*H*); ^{13}C NMR (75 MHz, $CDCl_3$ + DMSO-d_6): δ 56.1 (O*C*H_3), 60.9 (O*C*H_3), 104.6, 108.9, 114.7, 115.0, 118.6, 118.9, 119.5 (Ar–*C*), 130.1 (H*C*=CH), 132.6 (H*C*=CH), 132.7 (Ar*C*–Cl), 139.3 (*C*–OCH_3), 153.4 (*C*–OCH_3), 161.6 (*C*=N), 164.6(*C*=N), 165.5(Ar*C*–F) ppm; IR (KBr) (ν_{max}/cm^{-1}): $\nu = 3421$, 3067, 2924, 1733, 1637, 1585, 1503, 1464, 1416, 1333, 1244, 1200, 1126 cm^{-1}; MS (ESI) *m/z* 391; HR-MS (ESI) *m/z* for $C_{19}H_{17}N_2O_4FCl$ calculated *m/z*: 391.0860, found *m/z*: 391.0849.

*(E)-2-(5-bromopyridin-3-yl)-5-(3,4,5-trimethoxystyryl)-1,3,4-oxadiazole (**4m**)*

Yellow-colored crystals; (yield 256 mg, 29.23 %): $R_f = 0.4$ (50 % ethyl acetate/hexane); mp: 156–159 °C; ^{1}H NMR (300 MHz, $CDCl_3$); δ 3.91 (s, 3H, –OCH_3), 3.91 (s, 6H, –OCH_3), 6.83 (s, 2H, Ar*H*), 7.03 (d, 1H, $J = 15.8$ Hz, *trans*-C*H*=C*H*–), 7.60 (d, 1H, $J = 15.8$ Hz, *trans*-C*H*=C*H*–), 8.55 (s, 1H, Ar*H*), 8.87 (s, 1H, Ar*H*), 9.27 (s, 1H, Ar*H*); ^{13}C NMR (75 MHz; $CDCl_3$): δ 56.1 (O*C*H_3), 60.1 (O*C*H_3), 104.7, 108.4 (Ar–*C*), 129.8 (H*C*=CH), 136.1 (H*C*=CH), 140.0 (*C*–OCH_3), 145.6, 153.2 (Ar*C*–N), 153.4 (*C*–OCH_3), 160.5 (*C*=N), 164.9 (*C*=N) ppm; IR (KBr) (ν_{max}/cm^{-1}): $\nu = 3422$, 3042, 2928, 1734, 1638, 1579, 1518, 1455, 1415, 1330, 1243, 1186, 1125 cm^{-1}; MS (ESI) *m/z*: 418 [M$^+$], 420 [M^{2+}]; HR-MS (ESI) *m/z* for $C_{18}H_{19}N_3O_4Br$ calculated *m/z*: 418.0378, found *m/z*: 418.0386.

*(E)-2-(4-methoxyphenyl)-5-(3,4,5-trimethoxystyryl)-1,3,4-oxadiazole (**4n**)*

Light yellow-colored solid; (yield 526 mg, 68.06 %): $R_f = 0.6$ (50 % ethyl acetate/hexane); mp: 150–152 °C; ^{1}H NMR (300 MHz, $CDCl_3$); δ 3.91 (s, 3H, –OCH_3), 3.88 (s, 3H, –OCH_3), 3.91 (s, 6H, –OCH_3), 6.76 (s, 2H, Ar*H*), 6.95 (d, 1H, $J = 16.8$ Hz, *trans*-C*H*=C*H*–), 6.99 (d, 2H, $J = 8.9$ Hz, Ar*H*), 7.46 (d, 1H, $J = 16.8$ Hz, *trans*-C*H*=C*H*–), 8.01 (d, 1H, $J = 8.9$ Hz, Ar*H*); ^{13}C NMR (75 MHz; $CDCl_3$): δ 55.4 (O*C*H_3), 56.0 (O*C*H_3), 60.9(O*C*H_3), 104.4, 109.3, 114.4 (Ar–*C*), 130.3 (H*C*=CH), 128.6 (H*C*=CH), 138.1(*C*–OCH_3), 153.4 (*C*–OCH_3), 160.7 (*C*=N), 162.2 (*C*=N) ppm; IR (KBr) (ν_{max}/cm^{-1}): $\nu = 3427$, 2919, 2844, 1615, 1531, 1499, 1458, 1420, 1334, 1306, 1252, 1131, 1167 cm^{-1}; MS (ESI) *m/z*: 369 [M$^+$]; HR-MS (ESI) *m/z* for $C_{18}H_{19}N_3O_4Br$ calculated *m/z*: 369.1450 found *m/z*: 369.1446.

*(E)-2-(pyridin-3-yl)-5-(3,4,5-trimethoxystyryl)-1,3,4-oxadiazole (**4o**)*

Yellow-colored crystals; (yield 426 mg, 59.6 %): $R_f = 0.5$ (50 % ethyl acetate/hexane); mp: 136–139 °C; ^{1}H NMR (300 MHz, $CDCl_3$); δ 3.89 (s, 3H, –OCH_3), 3.93 (s, 6H, –OCH_3), 6.79 (s, 2H, Ar*H*), 7.02 (d, 1H, $J = 15.4$ Hz, *trans*-C*H*=C*H*–), 7.39–7.42 (m, 1H, $J = 3.6$ Hz, ArH), 7.51 (d, 1H, $J = 15.4$ Hz, *trans*-C*H*=C*H*–), 8.38 (d, 1H, $J = 7.2$ Hz, Ar*H*), 8.72 (d, 1H, $J = 4.5$ Hz, Ar*H*) 9.34 (s, 2H, Ar*H*); ^{13}C NMR (75 MHz, $CDCl_3$): δ 56.1 (O*C*H_3), 60.1 (O*C*H_3), 104.7, 108.4 (Ar–*C*), 124.2 (H*C*=CH), 129.4 (Ar–*C*–*N*), 133.4 (H*C*=CH), 138.1(*C*–OCH_3), 147.6 (Ar–*C*–*N*), 151.4 (*C*–OCH_3), 161.5 (*C*=N), 164.9 (*C*=N) ppm; IR (KBr) (ν_{max}/cm^{-1}): $\nu = 3418$, 2923, 2849, 1711, 1621,

1584, 1508, 1465, 1420, 1340, 1317, 1247, 1191, 1120 cm^{-1}; MS (ESI) *m/z*: 339 [M^+], HR-MS (ESI) *m/z* for $C_{18}H_{17}N_3O_4$ calculated *m/z*: 339.1208, found *m/z*: 339.1218.

*(E)-2-(2-benzo[d][1,3]dioxol-5-yl)vinyl)-5-(3-nitrophenyl)-1,3,4-oxadiazole (**5a**)*

Yellow-colored crystals; (yield 406 mg, 46.3 %): $R_f = 0.4$ (40 % ethyl acetate/hexane); mp: 152–155 °C; ^{1}H NMR (300 MHz, $CDCl_3$ + DMSO-d_6); δ 6.02 (s, 2H, OC*H*$_2$O), 6.79–6.96 (m, 2H, Ar*H*, $J = 17.1$ Hz, *trans*-C*H*=C*H*–), 7.01–7.17 (m, 2H, Ar*H*), 7.58–7.65 (m, 1H, $J = 16.2$ Hz, *trans*-C*H*=C*H*–), 7.69–7.85 (m, 1H, Ar*H*), 8.36–8.58 (m, 2H, $J =$ Ar*H*), 8.90 (d, 1H, $J = 8.7$ Hz Ar*H*); ^{13}C NMR (75 MHz, $CDCl_3$): δ 101.6 (O–*C*H$_2$–*O*), 110.2, 113.7, 117.3, 121.1 (Ar–*C*), 125.2 (H*C*=CH), 127.1, 130.1, 132.6 (Ar–*C*), 134.1 (H*C*=CH), 138.2 (Ar–*C*), 141.4 (Ar–*C*–*NO*$_2$), 149.0 (Ar–*C*–*O*), 149.6 (Ar–*C*–*O*), 161.0 (*C*=N), 163.8 (*C*=N) ppm; IR (KBr) (ν_{max}/cm^{-1}): $\nu = 3376$, 2924, 2853, 1741, 1705, 1632, 1554, 1523, 1496, 1450, 1345, 1262, 1174, 1103 cm^{-1}; MS (ESI) *m/z*: 337 [M^+], HR-MS (ESI) *m/z* for $C_{17}H_{12}N_3O_5$ calculated *m/z*: 339.0716, found *m/z*: 339.0720.

*(E)-2-(2-benzo[d][1,3]dioxol-5-yl)vinyl)-5-(2-chlorophenyl)-1,3,4-oxadiazole (**5b**)*

Yellow-colored crystals; (yield 537 mg, 63.3 %): $R_f = 0.5$ (40 % ethyl acetate/hexane); mp: 144–146 °C; ^{1}H NMR (300 MHz, $CDCl_3$); δ 6.02 (s, 2H, OC*H*$_2$O), 6.82 (d, 1H, $J = 8.3$ Hz, Ar*H*), 6.93 (d, 1H, $J = 15.4$ Hz, *trans*-C*H*=C*H*–), 7.03 (d, 1H, $J = 6.0$ Hz, Ar*H*), 7.08 (s, 1H, Ar*H*), 7.42 (d, 1H, $J = 15.8$ Hz, *trans*-C*H*=C*H*–), 7.39-7.98 (m, 3H, Ar*H*), 8.08 (d, 1H, $J = 7.5$ Hz, Ar*H*); ^{13}C NMR (75 MHz, $CDCl_3$): δ 101.3 (O–*C*H$_2$–*O*), 109.6, 111.4, 121.2 (Ar–*C*), 124.1 (H*C*=CH), 126.6, 127.5, 129.7 (Ar–*C*), 132.5 (Ar–*C*–Cl), 131.1 (Ar–*C*), 134.5 (H*C*=CH), 139.2, 140.3 (Ar–*C*), 149.7 (Ar–*C*–*O*), 148.4 (Ar–*C*–*O*), 162.1 (*C*=N), 164.9 (*C*=N), ppm; IR (KBr) (ν_{max}/cm^{-1}): $\nu = 3445$, 3070, 2918, 1634, 1598, 1522, 1495, 1446, 1353, 1256, 1101 cm^{-1}; MS (ESI) *m/z*: 327 [M^+], HR-MS (ESI) *m/z* for $C_{18}H_{17}N_3O_4$ calculated *m/z*: 327.0536, found *m/z*: 327.0544.

*(E)-2-(2-benzo[d][1,3]dioxol-5-yl)vinyl)-5-(4-nitrophenyl)-1,3,4-oxadiazole (**5c**)*

Yellow-colored solid; (yield 400 mg, 45.6 %): $R_f = 0.4$ (40 % ethyl acetate/hexane); mp: 152–154 °C; ^{1}H NMR (300 MHz, $CDCl_3$ + DMSO-d_6); δ 6.04 (s, 2H, OC*H*$_2$O), 6.77–6.93 (m, 1H, $J = 16.4$ Hz, *trans*-C*H*=C*H*), 7.02–7.11 (m, 1H, Ar*H*), 7.25 (s, 1H, Ar*H*), 7.55 (d, 1H, $J = 16.2$ Hz, *trans*-C*H*=C*H*), 8.17 (t, 1H, $J = 8.8$ Hz, Ar*H*), 8.29 (d, 1H, $J = 7.7$ Hz, Ar*H*), 8.36 (d, 2H, $J = 9.0$ Hz, Ar*H*), 8.44 (t, 1H, $J = 9.0$ Hz, Ar*H*); ^{13}C NMR (75 MHz, $CDCl_3$ + DMSO-d_6): δ 101.2 (O–*C*H$_2$–*O*), 111.6, 114.9, 118.9, 123.8 (Ar–*C*), 124.2 (H*C*=CH), 127.7, 128.0, 132.1 (Ar–*C*), 133.6 (H*C*=CH), 146.6 (Ar–*C*–*O*), 147.8 (Ar–*C*–*O*), 148.9 (Ar–*C*–*NO*$_2$), 161.8 (*C*=N), 163.5 (*C*=N) ppm; IR (KBr) (ν_{max}/cm^{-1}): $\nu = 3024$, 2926, 1752, 1695, 1630, 1544, 1502, 1492, 1482, 1292, 1266, 1202, 1154 cm^{-1}; MS (ESI) *m/z*: 337 [M^+], HR-MS (ESI) *m/z* for $C_{17}H_{12}N_3O_5$ calculated *m/z*: 339.0716, found *m/z*: 339.0720.

*(E)-2-(2-benzo[d][1,3]dioxol-5-yl)vinyl)-5-(3,4,5-trimethoxyphenyl)-1,3,4-oxadiazole (**5d**)*

Light yellow-colored solid; (yield 615 mg, 61.9 %): $R_f = 0.4$ (40 % ethyl acetate/hexane); mp: 149–152 °C; ^{1}H NMR (300 MHz, $CDCl_3$); δ 3.89 (s, 3H, OC*H*$_2$O), 3.96 (s, 6H, OC*H*$_3$), 6.02 (s, 2H, OC*H*$_2$O), 6.83 (d, 1H, $J = 7.9$ Hz, Ar*H*), 6.87 (d, 1H, $J = 15.8$ Hz, *trans*-C*H*=C*H*), 7.03 (d, 1H, $J = 7.9$ Hz, Ar*H*), 7.07–7.14 (m, 1H, Ar*H*), 7.30 (d, 2H, $J = 9.8$ Hz, Ar*H*), 7.50 (d, 1H, $J = 17.8$ Hz, *trans*-C*H*=C*H*); ^{13}C NMR (75 MHz, $CDCl_3$): δ 56.1 (OC*H*$_3$), 60.2 (OC*H*$_3$), 101.5 (O–*C*H$_2$–*O*), 103.9, 104.2, 106.0, 107.8, 108.4, 118.5 (Ar–*C*), 124.3(H*C*=CH), 129.1 (Ar–*C*), 138.8 (H*C*=CH), 148.8 (Ar–*C*–*O*), 148.0 (Ar–*C*–*O*), 153.4 (*C*–OCH$_3$), 162.9 (*C*=N), 164.1 (*C*=N) ppm; IR (KBr) (ν_{max}/cm^{-1}): $\nu = 3423$, 3050, 2928, 2834, 1638, 1583, 1453, 1420, 1247, 1132, 972 cm^{-1}; MS (ESI) *m/z*: 383 [M^+], HR-MS (ESI) *m/z* for $C_{20}H_{19}N_2O_6$ calculated *m/z*: 383.1206, found *m/z*: 383.1209.

*(E)-2-(2-(benzo[d][1,3]dioxol-5-yl)vinyl)-5-(3,4-dimethoxyphenyl)-1,3,4-oxadiazole (**5e**)*

Light yellow-colored solid; (yield 655 mg, 71.5 %): $R_f = 0.5$ (40 % ethyl acetate/hexane); mp: 143–145 °C; ^{1}H NMR (300 MHz, $CDCl_3$ + DMSO-d_6); δ 3.95 (s, 3H, OC*H*$_3$), 3.98 (s, 3H, OC*H*$_3$), 6.01 (s, 2H, OC*H*$_2$O), 6.82 (d, 1H, $J = 8.5$ Hz, Ar*H*), 6.89 (d, 1H, $J = 17.0$ Hz, *trans*-C*H*=C*H*), 6.95 (d, 1H, $J = 8.5$ Hz, Ar*H*), 7.03 (d, 1H, $J = 8.5$ Hz, Ar*H*), 7.07 (s, 1H, Ar*H*), 7.50 (d, 1H, $J = 17.0$ Hz, *trans*-C*H*=C*H*), 7.61–7.67 (m, 2H, $J = 8.5$ Hz, Ar*H*); ^{13}C NMR (75 MHz, $CDCl_3$ + DMSO-d_6): δ 55.3(OC*H*$_3$), 60.91 (OC*H*$_3$), 104.4 (O–*C*H$_2$–*O*), 109.5, 114.4, 116.2 (Ar–*C*), 128.6 (H*C*=CH), 130.3 (H*C*=CH), 138.1(*C*–OCH$_3$), 139.6 (Ar–*C*–*O*), 150.1 (Ar–*C*–*O*), 153.4 (*C*–OCH$_3$), 162.2 (*C*=N), 163.7 (*C*=N) ppm; IR (KBr) (ν_{max}/cm^{-1}): $\nu = 3418$, 2922, 2852, 1736, 1638, 1601, 1507, 1449, 1326, 1255, 1183, 1142, 1108 ppm; MS (ESI) *m/z*: 353 [M^+], HR-MS (ESI) *m/z* for $C_{19}H_{16}N_2O_5$ calculated *m/z*: 353.1176, found *m/z*: 353.1178.

*(E)-2-(2-benzo[d][1,3]dioxol-5-yl)vinyl)-5-(2,4-dichlorophenyl)-1,3,4-oxadiazole (**5h**)*

Yellow-colored solid; (yield 494 mg, 52.48 %): $R_f = 0.5$ (40 % ethyl acetate/hexane); mp: 162–164 °C; ^{1}H NMR (400 MHz, $CDCl_3$); δ 6.09 (s, 2H, OCH_2O), 6.90 (d, 1H, $J = 7.6$ Hz, Ar*H*), 6.93–6.98 (m, 1H, $J = 16.1$ Hz, *trans*-C*H*=C*H*), 7.09(d, 1H, $J = 7.6$ Hz, Ar*H*), 7.11 (s, 1H, Ar*H*), 7.41–7.50 (m, 1H, $J = 7.6$ Hz, Ar*H*), 7.56–7.66 (m, 2H, $J = 16.2$ Hz, *trans*-C*H*=C*H*), 8.10 (d, 1H, $J = 8.5$ Hz Ar*H*); ^{13}C NMR (75 MHz, $CDCl_3$): δ 101.4 (O–*C*H_2–*O*), 110.8, 113.6, 118.3 (Ar–*C*), 125.7 (H*C*=CH), 126.9, 129.0, 131.1 (Ar–*C*), 132.6 (Ar–*C*–Cl), 134.9 (H*C*=CH), 139.6 (Ar–*C*–Cl), 148.0 (Ar–*C*–*O*), 148.0 (Ar–*C*–*O*), 162.4(*C*=N), 164.4 (*C*=N) ppm; IR (KBr) (ν_{max}/cm^{-1}): $\nu = 3780$, 3693, 3409, 3075, 2920, 2852, 1732, 1635, 1595, 1523, 1493, 1450, 1408, 1356, 1261, 1103 cm^{-1}; MS (ESI) *m/z*: 361 [M$^+$], HR-MS (ESI) *m/z* for $C_{17}H_{11}N_3O_3Cl_2$ calculated *m/z*: 361.0146, found *m/z*: 361.0156.

*(E)-2-(2-benzo[d][1,3]dioxol-5-yl)vinyl)-5-(3-chloro-4-fluorophenyl)-1,3,4-oxadiazole (**5i**)*

Light yellow-colored solid; (yield 680 mg, 76.0 %): $R_f = 0.5$ (40 % ethyl acetate/hexane); mp: 172–175 °C; ^{1}H NMR (200 MHz, $CDCl_3$); δ 6.02 (s, 2H, OCH_2O), 6.77–6.92 (m, 2H, Ar*H*, $J = 16.6$ Hz, *trans*-C*H*=C*H*), 7.00–7.08 (m, 2H, Ar*H*), 7.23–7.35 (m, 1H, Ar*H*), 7.42–7.64 (m, 1H, $J = 15.8$ Hz, *trans*-C*H*=C*H*), 7.97–8.04 (m, 1H, Ar*H*), 8.06–8.17 (m, 1H, Ar*H*); ^{13}C NMR (75 MHz, $CDCl_3$): δ 101.4 (O–*C*H_2–*O*), 110.9, 116.6, 119.8 (Ar–*C*), 121.2 (Ar–*C*–Cl), 122.4 (Ar–*C*), 124.7 (H*C*=CH), 128.4, 129.4 (Ar–*C*), 131.6 (H*C*=CH), 148.2 (Ar–*C*–*O*), 149.7 (Ar–*C*–*O*), 161.4 (*C*=N), 162.1 (*C*=N), 164.8 (Ar–*C*–F) ppm; IR (KBr) (ν_{max}/cm^{-1}); $\nu = 3418$, 2922, 2853, 1714, 1636, 1603, 1492, 1447, 1358, 1259 cm^{-1}; MS(ESI) *m/z*: 345 [M$^+$], HR-MS(ESI) *m/z* for $C_{17}H_{11}N_2O_3ClF$ calculated *m/z*: 345.0421, found *m/z*: 345.0424.

*(E)-2-(2-benzo[d][1,3]dioxol-5-yl)vinyl)-5-(5-bromopyridin-3-yl)-1,3,4-oxadiazole (**5j**)*

Yellow-colored solid; (yield 298 mg, 30.0 %): $R_f = 0.4$ (40 % ethyl acetate/hexane); mp: 140–142 °C; ^{1}H NMR (300 MHz, $CDCl_3$ + DMSO-d_6); δ 6.03 (s, 2H, OCH_2O), 6.80 (d, 1H, $J = 8.3$ Hz, Ar*H*), 6.94 (d, 1H, $J = 15.8$ Hz, *trans*-C*H*=C*H*), 7.01–7.05 (m, 1H, $J = 6.7$ Hz, Ar*H*), 7.08 (s, 1H, ArH), 7.25 (s, 2H, Ar*H*), 7.50 (d, 1H, $J = 15.8$ Hz, *trans*-C*H*=C*H*), 8.46–8.49 (m, 1H, ArH), 8.75–8.81 (m, 1H, ArH), 9.18–9.22 (m, 1H, ArH); ^{13}C NMR (75 MHz, $CDCl_3$ + DMSO-d_{63}): δ 101.2 (O–*C*H_2–*O*), 111.5, 112.3, 114.6, 118.7, 121.6 (Ar–*C*), 122.4(Ar–*C*–Br), 126.1 (H*C*=CH), 128.5 (Ar–*C*), 134.5 (H*C*=CH), 146.6 (Ar–*C*–N), 148.1 (Ar–*C*–*O*), 148.6 (Ar–*C*–*O*), 162.2 (*C*=N), 164.5 (*C*=N) ppm; IR (KBr) (ν_{max}/cm^{-1}); $\nu = 3418$, 3028, 2921, 2853, 1709, 1609, 1500, 1443, 1365, 1311, 1260, 1211, 1155, 1100, 1040 cm^{-1}; MS (ESI) *m/z*: 373 [M$^+$], HR-MS (ESI) *m/z* for $C_{17}H_{10}N_3O_3Br$ calculated *m/z*: 373.9910, found *m/z*: 373.9920.

*(E)-2-(2-benzo[d][1,3]dioxol-5-yl)vinyl)-5-phenyl-1,3,4-oxadiazole (**5k**)*

Yellow-colored solid; (yield 244 mg, 32.1 %): $R_f = 0.4$ (40 % ethyl acetate/hexane); mp: 150–151 °C; ^{1}H NMR (200 MHz, $CDCl_3$); δ 6.02 (s, 2H, OCH_2O), 6.81 (d, 1H, $J = 8.3$ Hz, Ar*H*), 6.88 (d, 1H, $J = 15.8$ Hz, *trans*-C*H*=C*H*), 7.02 (d, 1H, $J = 1.5$ Hz, Ar*H*), 7.07 (s, 1H, Ar*H*), 7.47–7.55 (m, 4H, Ar*H*, $J = 15.8$ Hz, *trans*-C*H*=C*H*), 8.06–8.12 (m, 2H, Ar*H*); ^{13}C NMR (75 MHz, $CDCl_3$): δ 101.3 (O–*C*H_2–*O*), 112.5, 116.2, 119.7 (Ar–*C*), 124.7 (H*C*=CH), 127.1, 127.8, 128.6, 130.4, 131.1 (Ar–*C*), 135.4 (H*C*=CH), 148.7 (Ar–*C*–*O*), 148.2 (Ar–*C*–*O*), 162.0 (*C*=N), 164.5 (*C*=N) ppm; IR (KBr) (ν_{max}/cm^{-1}); $\nu = 3423$, 3080, 2919, 1733, 1641, 1603, 1493, 1447, 1358, 1260, 1099, 1030 cm^{-1}; MS (ESI) *m/z*: 293 [M$^+$], HR-MS (ESI) *m/z* for $C_{17}H_{13}N_3O_3$ calculated *m/z*: 293.0926, found *m/z*: 293.0914.

*(E)-2-(2-(benzo[d][1,3]dioxol-5-yl)vinyl)-5-(2-bromophenyl)-1,3,4-oxadiazole (**5l**)*

Light yellow-colored solid; (yield 459 mg, 47.7 %): $R_f = 0.5$ (40 % ethyl acetate/hexane); mp: 139–142 °C; ^{1}H NMR (300 MHz, $CDCl_3$); δ 6.02 (s, 2H, OCH_2O), 6.80 (d, 1H, $J = 7.9$ Hz, Ar*H*), 6.89 (d, 1H, $J = 16.4$ Hz, *trans*-C*H*=C*H*), 7.05 (d, 1H, $J = 8.1$ Hz, Ar*H*), 7.08 (s, 1H, Ar*H*), 7.34–7.41 (m, 4H, $J = 7.7$ Hz, Ar*H*), 7.42–7.54 (m, 2H, Ar*H*, $J = 16.4$ Hz, *trans*-C*H*=C*H*), 7.74 (d, 1H, $J = 7.9$ Hz, Ar*H*), 8.03–8.12 (m, 1H, ArH); ^{13}C NMR (75 MHz, $CDCl_3$): δ 101.5 (O–*C*H_2–*O*), 108.6, 105.9, 107.7, 121.4 (Ar–*C*), 123.7 (H*C*=CH), 127.5 (Ar–*C*–Br), 126.8, 129.0, 132.3, 131.55, 134.5 (H*C*=CH), 138.5, 139.1, 149.3 (Ar–*C*–*O*), 148.4 (Ar–*C*–*O*), 162.6 (*C*=N), 164.8 (*C*=N) ppm; IR (KBr) (ν_{max}/cm^{-1}); $\nu = 3430$, 2911, 1640, 1602, 1523, 1495, 1445, 1357, 1260, 1290, 1198, 1104, 1038 cm^{-1}; MS (ESI) *m/z*: 371 [M$^+$], HR-MS (ESI) *m/z* for $C_{17}H_{12}N_2O_3Br$ calculated *m/z*: 371.0031, found *m/z*: 371.0040.

*(E)-2-(2-benzo[d][1,3]dioxol-5-yl)vinyl)-5-(2-chloro-4-fluorophenyl)-1,3,4-oxadiazole (**5m**)*

Light yellow-colored solid; (yield 396 mg, 57.0 %): $R_f = 0.5$ (40 % ethyl acetate/hexane); mp: 165–167 °C; ^{1}H

NMR (300 MHz, $CDCl_3$ + DMSO-d_6); δ 6.05 (s, 2H, OCH_2O), 6.84 (d, 1H, J = 8.5 Hz, Ar*H*), 6.91–6.97 (m, 1H, J = 17.0 Hz *trans*-C*H*=C*H*), 7.06 (d, 1H, J = 6.8 Hz, Ar*H*), 7.12 (s, 1H, Ar*H*), 7.16–7.26 (m, 1H, Ar*H*), 7.33–7.37 (m, 1H, ArH), 7.56 (d, 1H, J = 17.0 Hz, *trans*-C*H*=C*H*); ^{13}C NMR (75 MHz, $CDCl_3$ + DMSO-d_6): δ 101.4 (O–*C*H_2–*O*), 110.9, 116.6, 119.8, 121.2, 122.4 (Ar–*C*), 124.1 (H*C*=CH), 128.2, 129.4 (Ar–*C*–Cl), 131.6 (H*C*=CH), 148.2(Ar–*C*–*O*), 149.7 (Ar–*C*–*O*), 161.4 (*C*=N), 162.1 (*C*=N), 164.8 (Ar–*C*–F) ppm; IR (KBr) (ν_{max}/cm^{-1}); ν = 3417, 2917, 1734, 1638, 1606, 1495, 1456, 1413, 1361, 1301, 1260, 1201, 1097 cm^{-1}; MS (ESI) *m/z*: 345 [M$^+$], HR-MS (ESI) *m/z* for $C_{17}H_{11}N_2O_3ClF$ calculated *m/z*: 345.0421, found *m/z*: 345.0424.

*(E)-2-(2-benzo[d][1,3]dioxol-5-yl)vinyl)-5-(2-chloropyridin-3yl)-1,3,4-oxadiazole (**5n**)*

Yellow-colored solid; (yield 470 mg, 55.0 %): R_f = 0.5 (40 % ethyl acetate/hexane); mp: 137–139 °C; ^{1}H NMR (400 MHz, $CDCl_3$); δ 6.05 (s, 2H, OCH_2O), 6.80 (d, 1H, J = 8.3 Hz, Ar*H*), 6.91–6.97 (m, 1H, J = 16.2 Hz, *trans*-C*H*=C*H*), 7.03 (d, 1H, J = 6.8 Hz, Ar*H*), 7.08 (s, 1H, Ar*H*), 7.16 (s, 2H, Ar*H*), 7.50 (d, 1H, J = 16.2 Hz, *trans*-C*H*=C*H*); ^{13}C NMR (75 MHz, $CDCl_3$): δ 101.2 (O–*C*H_2–*O*), 111.5, 112.3, 117.8, 118.0, 121.6 (Ar–*C*), 123.4 (H*C*=CH), 126.1, 128.5 (Ar–*C*), 134.5 (H*C*=CH), 146.6 (Ar–*C*–*N*), 148.1 (Ar–*C*–*O*), 148.5 (Ar–*C*–*O*), 162.2 (*C*=N), 164.5 (Ar–*C*–Cl) ppm; IR (KBr) (ν_{max}/cm^{-1}); ν = 3419, 3081, 2918, 1699, 1606, 1496, 1450, 1384, 1347, 1258, 1172, 1125, 1039 cm^{-1}; MS (ESI) *m/z*: 329 [M$^+$], HR-MS (ESI) *m/z* for $C_{16}H_{11}N_3O_3Cl$ calculated *m/z*: 329.0406, found *m/z*: 329.0416.

*(E)-2-(2-benzo[d][1,3]dioxol-5-yl)vinyl)-5-p-tolyl-1,3,4-oxadiazole (**5o**)*

Light yellow-colored solid; (yield 504 mg, 63.3 %): R_f = 0.4 (40 % ethyl acetate/hexane); mp: 158–160 °C; ^{1}H NMR (200 MHz, $CDCl_3$); δ 2.44 (s, 3H, –CH_3), 6.02 (s, 2H, OCH_2O), 6.82 (d, 1H, J = 8.3 Hz, Ar*H*), 6.87(d, 1H, J = 15.8 Hz, *trans*-C*H*=C*H*), 7.02 (d, 1H, J = 7.5 Hz, Ar*H*), 7.06 (s, 1H, Ar*H*), 7.28 (d, 2H, J = 7.5 Hz, Ar*H*), 7.50 (d, 1H, J = 16.2 Hz, *trans*-C*H*=C*H*), 7.96(d, 2H, J = 8.3 Hz, Ar*H*); ^{13}C NMR (75 MHz, $CDCl_3$): δ 26.3 (–*C*H_3), 101.3 (O–*C*H_2–*O*), 110.5, 114.3, 119.7, 122.2 (Ar–*C*), 125.0 (H*C*=CH), 126.9, 127.4, 128.5, 129.7, 130.8 (Ar–*C*), 134.5 (H*C*=CH), 139.6 (Ar–*C*), 147.9 (Ar–*C*–*O*), 148.4 (Ar–*C*–*O*), 162.1 (*C*=N), 164.5 (*C*=N) ppm; IR (KBr) (ν_{max}/cm^{-1}); ν = 3782, 3692, 3631, 3428, 2919, 1731, 1631, 1604, 1492, 1524, 1444, 1355, 1312, 1254 cm^{-1}; MS (ESI) *m/z*: 307 [M$^+$], HR-MS (ESI) *m/z* for $C_{18}H_{15}N_2O_3$ calculated *m/z*: 307.1082, found *m/z*: 307.1095.

*(E)-2-(2-benzo[d][1,3]dioxol-5-yl)vinyl)-5-(pyridin-3yl)-1,3,4-oxadiazole (**5p**)*

Yellow-colored crystals; (yield 358 mg, 46.8 %): R_f = 0.5 (40 % ethyl acetate/hexane); mp: 126–128 °C; ^{1}H NMR (200 MHz, $CDCl_3$); δ 6.02 (s, 2H, OCH_2O), 6.82 (d, 1H, J = 8.1 Hz, Ar*H*), 6.94 (d, 1H, J = 15.3 Hz, *trans*-C*H*=C*H*), 7.03 (d, 1H, J = 8.1 Hz, Ar*H*), 7.09 (s, 1H, Ar*H*), 7.38–7.41 (m, 1H, Ar*H*), 7.50 (d, 1H, J = 15.8 Hz, *trans*-C*H*=C*H*), 8.36 (d, 2H, J = 8.1 Hz, Ar*H*), 8.72(d, 1H, J = 4.7 Hz, Ar*H*), 9.32(s, 1H, Ar*H*); ^{13}C NMR (75 MHz, $CDCl_3$): δ 101.2 (O–*C*H_2–*O*), 110.6, 114.2, 120.0 (Ar–*C*), 124.3(H*C*=CH), 125.0, 127.9 (Ar–*C*), 133.2 (Ar–*C*–*N*), 134.9 (H*C*=CH), 148.2 (Ar–*C*–*O*), 149.8 (Ar–*C*–*O*), 162.5 (*C*=N), 164.3 (*C*=N) ppm; IR (KBr) (ν_{max}/cm^{-1}); ν = 3419, 2921, 2853, 1613, 1596, 1500, 1450, 1417, 1363, 1317, 1265, 1207, 1182, 1105, 1033 cm^{-1}; MS (ESI) *m/z*:294 [M$^+$], HR-MS (ESI) *m/z* for $C_{18}H_{15}N_2O_3$ calculated *m/z*: 294.0806, found *m/z*: 294.0820.

*(E)-2-(2-benzo[d][1,3]dioxol-5-yl)vinyl)-5-(4-methoxyphenyl)-1,3,4-oxadiazole (**5q**)*

Yellow-colored crystals; (yield 341 mg, 40.7 %): R_f = 0.5 (40 % ethyl acetate/hexane); mp: 145–147 °C; ^{1}H NMR (300 MHz, $CDCl_3$); δ 3.89 (s, 3H, OCH_3), 6.03 (s, 2H, OCH_2O), 7.02–7.09 (m, 4H, Ar*H*), 7.50 (d, 1H, J = 15.8 Hz, *trans*-C*H*=C*H*), 7.94 (d, 1H, J = 9.0 Hz, Ar*H*), 8.02–8.08 (m, 3H, Ar*H*, J = 15.8 Hz, *trans*-C*H*=C*H*); ^{13}C NMR (75 MHz, $CDCl_3$): δ 56.0, 102.0 (O–*C*H_2–*O*), 111.6, 114.8, 115.7, 118.7, 119.0(Ar–*C*), 123.6 (H*C*=CH), 129.0, 129.7, 128.3 (Ar–*C*), 133.4 (H*C*=CH), 148.6 (Ar–*C*–*O*), 148.0 (Ar–*C*–*O*), 159.8 (Ar–*C*–OCH_3), 162.3 (*C*=N), 164.6 (*C*=N) ppm; IR (KBr) (ν_{max}/cm^{-1}); ν = 3422, 2925, 2856, 1735, 1622, 1450, 1257, 1170, 1031 cm^{-1}; MS (ESI) *m/z*: 283 [M$^+$], HR-MS (ESI) *m/z* for $C_{19}H_{13}N_2O_4$ calculated *m/z*: 283.1109, found *m/z*: 283.1107.

In vitro acetylcholinesterase (AChE) assay

AChE inhibitory assay was performed in 96-well microtiter plates based on the modified method of Ellman et al. (1961). The enzyme hydrolyzed the substrate acetylthiocholine resulting in the product thiocholine which reacts with Ellman's reagent (5,5′-dithio-bis-2-nitrobenzoic acid, DTNB) in situ and gives the yellow-colored chromophore of 5-thio-2-nitrobenzoic acid (TNB) which can be detected at 405 nm. The absorption intensity of TNB adduct (405 nm) is proportional to the formation of thiocholine; therefore, the AChE activity. In each well of the 96-well microtiter plate, 5 µl of compound and 10 µl of 0.01 U ml^{-1} of AChE (*Electrophorus electricus* AChE

Type VI-S, EC 3.1.1.7, Sigma) were incubated at 4 °C for 20 min before the addition of 10 µl of 1.5 mM ATCI in phosphate buffer (pH 7.5), 60 µl of 3 mM DTNB in phosphate buffer (pH 7.5), and 60 µl of 0.1 M phosphate buffer (pH 7.5) and absorbance was measured at 405 nm every 30 s for 4 min × 8 times on a TRIAD multimode reader (Dynex Technologies, Inc., Chantilly, VA, USA). The rate of reactions was calculated using the Manager software of the multimode reader. Percentage of inhibition was calculated by comparing the rates for each sample with respect to the blank (10 % DMSO in buffer). Galanthamine hydrobromide (0.1 µM ml^{-1}) as well as donepezil (0.1 µM ml^{-1}), both in DMSO solvent were used as positive controls. Each assay was performed in triplicate and the AChE inhibitory values are the average of three independent experiments.

AChE inhibitor galanthamine (a reversible cholinesterase inhibitor) was used in the concentration range of 0.1–100 µM to inhibit AChE of electric eel. The stock solutions of the (*E*)-2-aryl-5-styryl-1,3,4-oxadiazole derivatives were prepared based on the molecular weight of the individual compounds being dissolved in DMSO and to get the concentration of the original stock solution equivalent to 1000 µM in DMSO. This stock solution was further diluted to get the compound dilutions from 0.1, 1.0, 10, 50, and 100 µM per 5 µl of DMSO. Inhibition by (E)-2-aryl-5-styryl-1,3,4-oxadiazole derivatives was studied in the presence of different concentrations of compounds and the percentage inhibition of enzyme activity was calculated. The inhibition of AChE by **4**(**a**–**o**) and (**5a**–**q**) derivatives was analyzed in terms of IC_{50} values in µM obtained in comparison to that of galanthamine.

Molecular docking studies

Molecular docking studies were performed using GOLD (version 3.2) program protocol on the 1,3,4-oxadiazole derivatives with well-known complex acetylcholinesterase complexed with donepezil ligand which is marketed as Aricept (PDBID: 1EVE) which is downloaded from the RCSB protein data bank (Kryger *et al*., 1999; Badrinarayan *et al*., 2011; Badrinarayan and Sastry, 2011). The Accelrys Discovery studio protein preparation wizard was used to prepare the protein with default settings. The ligands were subjected to energy minimization at AM1 level of theory. The default parameters in GOLD 3.2, such as number of islands 5, population size 100, number of operations 100,000, niche size 2, selection pressure 1, the van der Waals and hydrogen bonding set to 4.0 and 2.5, respectively, were used to perform GOLD docking calculations (Ravindra *et al*., 2008; Srivastava *et al*., 2011). The binding site in AutoDock is defined by the grid of interaction points. The atom number 1280, the hydrogen atom of the active site residue Trp84 was defined as the center of grid, and the grid was made up of the grid points 70(*X*), 80(*Y*), and 126(*Z*) with grid spacing of 0.375 Å. The number of generations, energy evaluations, and individuals in the population are set to 27000, 5×10^6, and 150, respectively. The 50°/step was used for quaternion and torsion, while 2 Å/step was used for the translation during the docking run. The Lamarckian genetic algorithm was adopted for sampling ligand conformations. The default parameters of free energy scoring function were used for the docking studies (Srivastava *et al*., 2011).

Results and discussion

The synthesis of (*E*)-2-aryl-5-styryl-1,3,4-oxadiazole derivatives **4**(**a**–**o**) and **5**(**a**–**q**) described in the study are outlined in Scheme 1 and the structural data are presented in Table 1. Different aryl esters **7**(**a**–**q**) were synthesized by esterification of substituted aryl carboxylic acids **6**(**a**–**q**) in the presence of H_2SO_4 (catalyst) in ethanol. The esters were washed with saturated $NaHCO_3$ solution to afford pure carboxylic acid esters. In the next step, these synthesized esters were converted to their corresponding hydrazides **8**(**a**–**q**) on refluxing with hydrazine hydrate in ethanol. These hydrazides were cyclized with 3,4,5-trimethoxycinnamic acid or 3,4-(methylenedioxy)cinnamic acid in the presence of phosphorus oxychloride on refluxing for 5–6 h to afford the desired (*E*)-2-aryl-5-styryl-1,3,4-oxadiazole derivatives **4**(**a**–**o**) and **5**(**a**–**q**), respectively, in good yields. The purity of all the synthesized compounds was examined by TLC and their corresponding spectral data were recorded for ^1H and ^{13}C NMR, FT-IR, and HR-MS which confirmed the proposed structures.

The effect on AChE inhibition of these compounds with various substituents in the aryl ring is shown in Table 1. Among the 30 synthesized compounds, four compounds such as **4a**, **4g**, **5c**, and **5m** showed promising inhibitory activity with the IC_{50} values 24.89, 13.72, 37.65, and 19.63 µM, respectively. The compounds **5c**, **5d**, **5e**, **5l**, **5g**, **5b**, **5a**, **5h**, **5k**, **5j**, **5p**, **5n**, and **4h** exhibited moderate inhibitory activity, while the remaining synthesized compounds showed less to moderate inhibitory activity. The inhibition of enzyme activity increased proportionately with an increase in concentration for the two most promising compounds of each group (**4a**, **4g** and **5c**, **5m**). The presence of five-membered heterocyclic moiety (**4g**) at position C2 of oxadiazole ring showed more inhibition than the phenyl group (**4a**). The compound having 2-chloro-4-fluorophenyl at position C2 and 3,4-(methylenedioxy)styryl group at position C5 of oxadiazole (**5m**) showed significant inhibition when compared to other compounds in the same series. The compounds **5m** and **5c** were more active than

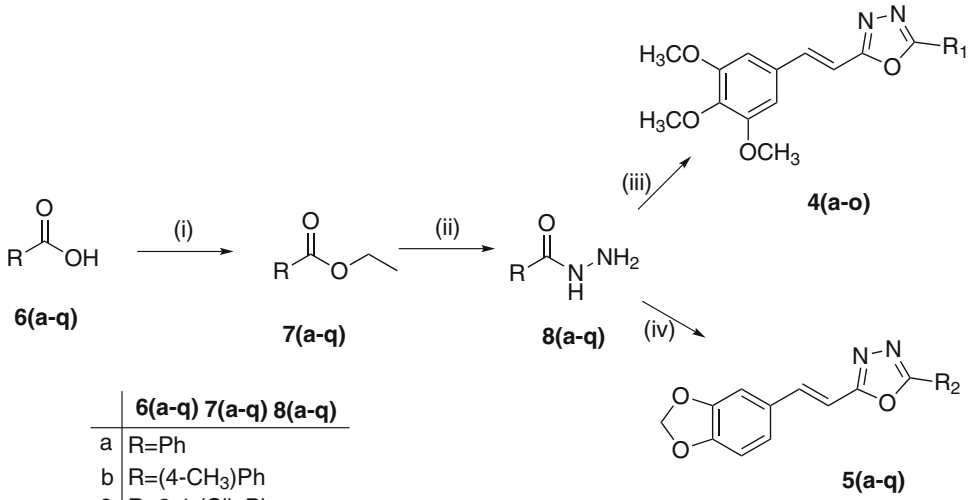

	6(a-q) 7(a-q) 8(a-q)
a	R=Ph
b	R=(4-CH_3)Ph
c	R=2,4-$(Cl)_2$Ph
d	R=(2-Cl)Py
e	R=(2-Br)Ph
f	R=2-BenFur
g	R=2-Fur
h	R=(4-NO_3)Ph
i	R=3,4,5$(OCH_3)_3$Ph
j	R=(3-NO_2)Ph
k	R=(2-Cl)Ph
l	R=(2-Cl,4-F)Ph
m	R=(5-Br)Py
n	R=(4-OCH_3)Ph
o	R=Py
q	R=3,4$(OCH_3)_2$Ph
p	R=(3-Cl,4-F)Ph

	4(a-o)		5(a-q)
a	R_1=Ph	a	R_2=(3-NO_2)Ph
b	R_1=(4-CH_3)Ph	b	R_2=(2-Cl)Ph
c	R_1=2,4-$(Cl)_2$Ph	c	R_2=(4-NO_2)Ph
d	R_1=(2-Cl)Py	d	R_2=3,4,5$(OCH_3)_3$Ph
e	R_1=(2-Br)Ph	e	R_2=3,4$(OCH_3)_2$Ph
f	R_1=2-BenFur	h	R_2=2,4-$(Cl)_2$Ph
g	R_1=2-Fur	i	R_2=(3-Cl,4-F)Ph
h	R_1=(4-NO_2)Ph	j	R_2=(5-Br)Py
i	R_1=3,4,5$(OCH_3)_3$Ph	k	R_2=Ph
j	R_1=(3-NO_2)Ph	l	R_2=(2-Br)Ph
k	R_1=(2-Cl)Ph	m	R_2=(3-Cl,4-F)Ph
l	R_1=(2-Cl,4-F)Ph	n	R_2=(2-Cl)Py
m	R_1=(5-Br)Py	o	R_2=(4-CH_3)Ph
n	R_1=(4-OCH_3)Ph	q	R_2=Py
o	R_1=Py	p	R_2=(4-OCH_3)Ph

Scheme 1 Synthesis of (*E*)-2-aryl-5-styryl-1,3,4-oxadiazole **4**(**a**–**o**) and **5**(**a**–**q**): reagents and conditions: (i) H_2SO_4 (catalyst)/EtOH, 3–4 h, reflux, (80–90 %); (ii) NH_2–NH_2·H_2O/EtOH, 3–4 h, reflux, (72–79 %); (iii) $POCl_3$, 5–6 h, 110 °C, (51–70 %); 3,4,5-trimethoxycinnamic acid or 3,4-(methylenedioxy)cinnamic acid. Note: *Ph* phenyl, *Py* pyridyl, *Fur* furyl, *BenFur* benzofuryl

compound **4a** which is due to the presence of electron-withdrawing groups like (NO_2) and (Cl and F) in **5c** and **5m**, respectively. The compounds with the presence of high electronegative groups like chlorine and fluorine at positions C2 and C4 in the phenyl ring (**5m**) were more active as compared to positions C3 and C4 in the phenyl ring (**5i**). Overall, the synthesized compounds showed good to moderate inhibitory activity with IC_{50} values ranging from 13 to 65 μM. The compounds in the series **5**(**a**–**q**) that contained the 3,4-(methylenedioxy) group at position C5 showed better activity than the compounds in the series **4**(**a**–**q**) that contained 3,4,5-trimethoxystyryl group (except compounds **4a** and **4g**). The two most promising compounds of each group (**4a**, **4g** and **5c**, **5m**) were further subjected to molecular docking studies to investigate their inhibition pattern.

The molecular docking studies have been carried out to evaluate the binding affinity between 1,3,4-oxadiazole derivatives and AChE enzyme using GOLD (version 3.2) docking software. The docking studies have been performed on four promising molecules **4a**, **4g**, **5c**, and **5m** with well-known acetylcholinesterase with donepezil which is marketed as Aricept (PDBID: 1EVE). The protein crystal structure has been retrieved from RCSB protein data bank. The AChE protein structure is available from two different sources of organisms, namely *Electrophorus electricus* and *Torpedo californica*, in the protein data bank. However, there is no ligand–enzyme complex reported for *Electrophorus electricus* AChE (Ee AChE). Hence, the *Torpedo californica* AChE (Tc AChE) ligand–enzyme complex 1EVE has been used for the molecular docking studies. The characteristic difference between these two enzymes is the replacement of Phe330 in Tc AChE with Tyr337 in Ee AChE. The active site radius was set to 10 Å from the atom number 1280, the hydrogen atom of the active site residue Trp84, which forms hydrophobic

Table 1 Structures of compounds **4**(**a**–**o**) and **5**(**a**–**q**) and their in vitro AChE inhibitory activities

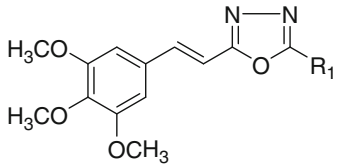

4(a-o)

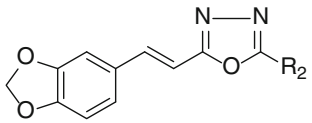

5(a-q)

Compound	R_1	IC_{50} value (μM, mean ± SE)	Compound	R_2	IC_{50} value (μM, mean ± SE)
4a	Ph	24.89 ± 0.03	**5a**	(3-NO_2)Ph	49.36 ± 0.01
4b	(4-CH_3)Ph	60.21 ± 0.03	**5b**	(2-Cl)Ph	47.42 ± 0.03
4c	2,4-$(Cl)_2$Ph	62.22 ± 0.01	**5c**	(4-NO_2)Ph	37.62 ± 0.02
4d	(2-Cl)Py	61.21 ± 0.04	**5d**	3,4,5$(OCH_3)_2$Ph	48.56 ± 0.05
4e	(2-Br)Ph	64.92 ± 0.06	**5e**	3,4$(OCH_3)_3$Ph	40.52 ± 0.03
4f	2-BenFur	60.43 ± 0.02	**5h**	2,4-$(Cl)_2$Ph	50.28 ± 0.03
4g	2-Fur	13.72 ± 0.01	**5i**	(3-Cl,4-F)Ph	49.64 ± 0.03
4h	(4-NO_2)Ph	49.01 ± 0.07	**5j**	(5-Br)Py	52.53 ± 0.08
4i	3,4,5$(OCH_3)_3$Ph	61.50 ± 0.03	**5k**	Ph	50.10 ± 0.03
4j	(3-NO_2)Ph	65.79 ± 0.03	**5l**	(2-Br)Ph	40.18 ± 0.03
4k	(2-Cl)Ph	58.07 ± 0.02	**5m**	(2-Cl,4-F)Ph	19.63 ± 0.01
4l	(2-Cl,4-F)Ph	60.23 ± 0.03	**5n**	(2-Cl)Py	54.33 ± 0.06
4m	(5-Br)Py	62.75 ± 0.02	**5o**	(4-CH_3)Ph	45.31 ± 0.01
4n	(4-OCH_3)Ph	61.21 ± 0.02	**5p**	Py	48.52 ± 0.04
4o	Py	65.01 ± 0.03	**5q**	(4-OCH_3)Ph	42.76 ± 0.02
Galanthamine (control)		4.420 ± 0.06			

Ph phenyl, *Py* pyridyl, *Fur* furyl, *BenFur* benzofuryl

π–π interactions with donepezil. The default parameters were used for docking in the GOLD software. The cross-validation of the GOLD docking results has been carried out using another docking protocol AutoDock. Results of both the docking methods followed same trends (Table 2). Thus, we have used GOLD results for the discussion in this manuscript. From the GOLD software results, it is obvious that these ligands showed very close docking scores when compared with donepezil ligand (58.16). The GOLD docking results (Table 3) depicted **4g** as the best active compound among the four ligands, which showed excellent biological activity with IC_{50} value of 13 μM among all compounds. The interactions of ligands in the binding site have been depicted in Fig. 2. In active site the best ranking compound **4g** (GOLD score 55.09) showed hydrophobic CH–π and π–π interactions with TRP84 and HIS440 residues, respectively. The diazole ring showed a strong cation–π type interaction with TYR334 residue (Fig. 2), which is absent in the remaining ligands. The hydrophobic π–π, CH–π, hydrogen bonding, and electrostatic interactions in active site made **4g** ligand as the most active compound. The ligand **5m** (GOLD score 54.08) depicted

Table 2 The docking results of (*E*)-2-aryl-5-styryl-1,3,5-oxadiazole derivatives using acetylcholinesterase enzyme (PDBID: 1EVE) with GOLD and AutoDock softwares

Ligand name	GOLD	AutoDock
4g	55.09	596.08
4a	51.19	452.90
5m	54.08	551.37
5c	51.99	470.31
Donepezil	58.16	642.75

Table 3 The GOLD docking results of (*E*)-2-aryl-5-styryl-1,3,5-oxadiazole derivatives using acetylcholinesterase enzyme (PDBID: 1EVE)

Ligand name	Fitness	Fitness rank	Hb_ext	vdw_ext	Int
4g	55.09	1	6.00	31.70	−8.36
4a	51.19	4	6.00	34.49	−6.14
5m	54.08	2	1.97	42.18	−3.3
5c	51.99	3	2.00	45.15	−5.41
Donepezil	58.16	1	0.08	50.03	−10.72

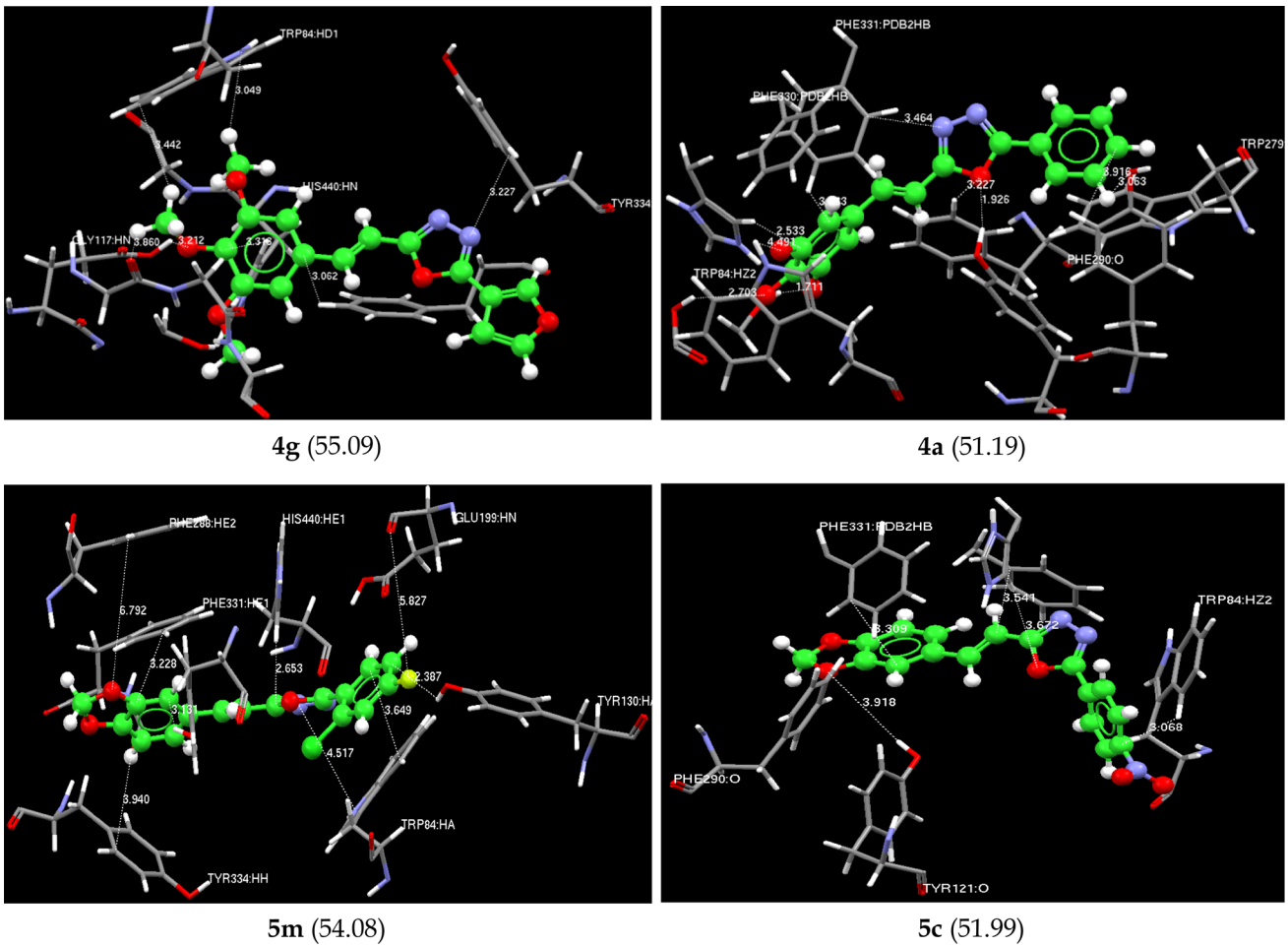

4g (55.09) **4a** (51.19)

5m (54.08) **5c** (51.99)

Fig. 2 The docked poses of the compounds in the active site of acetylcholinesterase enzyme (PDBID: 1EVE) and score in the *parenthesis* using GOLD protocol. Various non-covalent interactions and hydrogen bonding interactions showed in *dotted lines*

strong hydrophobic interactions with PHE331, HIS440, and TRP84 residues in the active site. Beside these interactions, the **5m** ligand showed CH–π and CH–O interactions with TYR334 and PHE290 residues, respectively (Fig. 2). The electrostatic (cation–π) type of interaction between the diazole and TYR334 residue (ligand **4g**) was absent in case of ligand **5m**. The compounds **4a** and **5c** also showed similar type of interactions; however, these ligands had less interactions when compared to the above two compounds (Fig. 2). The lack of hydrophobic and hydrogen bonding interactions made these ligands lesser active than other ligands. All the above-mentioned interactions are in the range <4.0 Å distance between ligand and binding site residues. Similar to the donepezil, the 1,3,4-oxadiazole derivatives showed a strong interaction with one face of the benzyl ring and displayed a classic parallel π–π stacking with the six-membered ring of the TRP84 indole. In conclusion, the docking results included hydrophobic and electrostatic interactions with binding site (TRP84, HIS440, and TYR334) amino acid residues and conventional hydrogen bonds at the bottom of the gorge were observed. These types of interactions were already known for other crystallized inhibitors of AChE (e.g., donepezil and galanthamine) and, therefore, the docking results were likely to be meaningful for the tested ligands. Moreover, all compounds were potentially able to bind inside the active side.

Conclusion

In our study, we have described for the first time the synthesis, biological evaluation, and molecular modeling of (*E*)-2-aryl-5-styryl-1,3,4-oxadiazole derivatives as AChE inhibitors. All the compounds showed good to moderate AChE inhibitory activity with IC_{50} values in the range of 13–65 μM. Based on molecular modeling results it was observed that the compounds **4a**, **4g**, **5c**, and **5m** bind to the AChE enzyme in a similar manner as donepezil. The strong hydrophobic interactions between the ligand and aromatic

amino acids are responsible for the activity of these compounds similar to donepezil ligand interactions. This investigation provided an insight for the future direction in the development of conjugates such as potential AChE inhibitors.

Acknowledgments The authors A. B. S. and G. N. R are thankful to CSIR, New Delhi, for the award of research fellowships.

Conflict of interest None.

References

Alam MM, Shaharyar M, Hamid H, Nazreen S, Haider S, Alam MS (2011) Synthesis of novel 8-hydroxy quinolin based 1,3,4-oxadiazoles and *S*-substituted 1,2,4-triazole derivatives and evaluation of their anti-inflammatory, analgesic, ulcerogenic and anti-microbial activities. Med Chem 7(6):663–673

Al-Kazzaz FF, Al-Hasani RAM, Zyzaffon N (2011) Sensitivity of serum acetylcholine esterase toward derivatives of oxadiazole. Eng Tech J 29(4):651–664

Alvarez A, Opazo C, Alarcon R, Garrido J, Inestrossa NC (1997) Acetylcholinesterase promotes the aggregation of amyloid-beta-peptide fragments by forming a complex with the growing fibrils. J Mol Biol 272(3):348–361

Alvarez A, Alarcon R, Opazo C, Campos EO, Munoz FJ, Calderon FH, Dajas F, Gentry MK, Doctor PB, De Mello FG, Inestrosa NC (1998) Stable complexes involving acetylcholinesterase and amyloid-beta peptide change the biochemical properties of the enzyme and increase the neurotoxicity of Alzheimer's fibrils. J Neurosci 18(9):3213–3223

Andreani A, Cavalli A, Granaiola M, Guardigli M, Leoni A, Locatelli A, Morigi R, Rambaldi M, Recanatini M, Roda AJ (2001) Synthesis and screening for antiacetylcholinesterase activity of (1-benzyl-4-oxopiperidin-3-ylidene)methylindoles and -pyrroles related to donepezil. J Med Chem 44(23):4011–4014

Badrinarayan P, Sastry GN (2011) Sequence, structure, and active site analyses of p38 MAP kinase: exploiting DFG-out conformation as a strategy to design new type II leads. J Chem Inf Model 51(1):115–129

Badrinarayan P, Srivani P, Sastry GN (2011) Design of 1-arylsulfamido-2-alkylpiperazine derivatives as secreted PLA2 inhibitors. J Mol Model 17(4):817–831

Bartus RT, Dean RLR, Beer B, Lippa AS (1982) The cholinergic hypothesis of geriatric memory dysfunction. Science 217(4558):408–414

Bhattacharya J, Patel K, Tailor P, Karthikeyan C, Moorthy NSH, Trivedi P (2010) Design, synthesis and characterization of novel 1,3,4-oxadiazole dimmers from benzoic acids. Int J Chem Technol Res 2:2055–2062

Davis KL, Powchik P (1995) Tacrine. Lancet 45(8950):625–630

De Ferrari GV, Canales MA, Shin I, Weiner LM, Silman I, Inestrosa NC (2001) A structural motif of acetylcholinesterase that promotes amyloid beta-peptide fibril formation. Biochemistry 40(35):10447–10457

Ellman GL, Courtney KD, Andres V Jr, Featherstone RM (1961) A new and rapid colorimetric determination of acetylcholinesterase activity. Biochem Pharmacol 7:88–95

Gaonkar SL, Rai KM, Prabhuswamy B (2006) Synthesis and antimicrobial studies of a new series of 2-[4-[2-(5-ethylpyridin-2-yl)ethoxy]phenyl]-5-substituted-1,3,4-oxadiazoles. Eur J Med Chem 41(7):841–846

Jha KK, Samad A, Kumar Y, Shaharyar M, Khosla RL, Jain J, Kumar V, Singh P (2010) Design, synthesis and biological evaluation of 1,3,4-oxadiazole derivatives. Eur J Med Chem 45(11):4963–4967

Johansson M, Hellström-Lindahl E, Nordberg A (1996) Steady-state pharmacokinetics of tacrine in long-term treatment of Alzheimer patients. Dementia 7(2):111–117

Kawakami Y, Inoue A, Kawai T, Wakita M, Sugimoto H, Hopfinger AJ (1996) The rationale for E2020 as a potent acetylcholinesterase inhibitor. Bioorg Med Chem 4(9):1429–1446

Kryger G, Silman I, Sussman JL (1999) Structure of acetylcholinesterase complexed with E2020 (Aricept): implications for the design of new anti-Alzheimer drugs. Structure 7(3):297–307

Lee L, Robb LM, Lee M, Davis R, Mackay H, Chavda S, Babu B, O'Brien EL (2010) Design, synthesis, and biological evaluations of 2,5-diaryl-2,3-dihydro-1,3,4-oxadiazoline analogs of combretastatin-A4. J Med Chem 53(1):325–334

Narayana B, Vijayaraj KK, Ashalata BV, Kumari NS (2005) Synthesis of some new 2-(6-methoxy-2-naphthyl)-5-aryl-1,3,4-oxadiazoles as possible non-steroidal anti-inflammatory and analgesic agents. Arch Pharm (Weinheim) 338(8):373–377

Prous J, Rabasseda X, Castaner J (1996) Cognition enhancer acetylcholinesterase inhibitor. Drugs Future 19(7):656–658

Rainer M (1997) Galanthamine in Alzheimer's disease: a new alternative to tacrine? CNS Drugs 7(2):89–97

Ravindra GK, Achaiah G, Sastry GN (2008) Molecular modeling studies of phenoxypyrimidinyl imidazoles as p38 kinase inhibitors using QSAR and docking. Eur J Med Chem 43(4):830–838

Shi W, Qian X, Zhang R, Song G (2001) Synthesis and quantitative structure-activity relationships of new 2,5-disubstituted-1,3,4-oxadiazoles. J Agric Food Chem 49(1):124–130

Singh P, Sharma PK, Sharma JK, Upadhyay A, Kumar N (2012) Synthesis and evaluation of substituted diphenyl-1,3,4-oxadiazole derivatives for central nervous system depressant activity. Org Med Chem Lett 2:8. doi:10.1186/2191-2858-2-8

Srivastava HK, Chourasia M, Kumar D, Sastry GN (2011) Comparison of computational methods to model DNA minor groove binders. J Chem Inf Model 51(3):558–571

Tan TM, Chen Y, Kong KH, Bai J, Li Y, Lim SG, Ang TH, Lam Y (2006) Synthesis and the biological evaluation of 2-benzenesulfonylalkyl-5-substituted-sulfanyl-[1,3,4]-oxadiazoles as potential anti-hepatitis B virus agents. Antiviral Res 71(1):7–14

Wagstaff AJ, McTavish D (1994) Tacrine. A review of its pharmacodynamic and pharmacokinetic properties, and therapeutic efficacy in Alzheimer's disease. Drugs Aging 4(6):510–540

Zarghi A, Tabatabai SA, Faizi M, Ahadian A, Navabi P, Zanganeh V, Shafiee A (2005) Synthesis and anticonvulsant activity of new 2-substituted-5-(2-benzyloxyphenyl)-1,3,4-oxadiazoles. Bioorg Med Chem Lett 15(7):1863–1865